Korean J. Chem. Eng., **29**(10), 1329-1335 (2012)
DOI: 10.1007/s11814-012-0057-5

Carbon dioxide reforming of methane to synthesis gas over $LaNi_{1-x}Cr_xO_3$ perovskite catalysts

Joonho Kim*, Taeyoon Kim*, Jung Whan Yoo, Ki Bong Lee*,†, and Suk-In Hong*,†**

*Department of Chemical and Biological Engineering, Korea University, Anam-dong, Seongbuk-gu, Seoul 136-713, Korea
**Eco-Composite Materials Center, Korea Institute of Ceramic Engineering and Technology, Gasan-dong, Guemcheon-gu, Seoul 153-801, Korea
(*Received 25 January 2012 • accepted 27 April 2012*)

Abstract−Carbon dioxide reforming of methane was investigated over $LaNi_{1-x}Cr_xO_3$ perovskite catalysts which were prepared by the malic acid method. The respective perovskite catalysts were a single phase of perovskite oxide without impurity phases. Their reduction behavior was characterized by temperature programmed reduction. In the $LaNi_{1-x}Cr_xO_3$ perovskite catalysts, the catalytic activities were closely related to the reduction behavior of the catalysts, and the partial substitution of Cr to the B-site of perovskite catalysts promoted stability against reduction. When the x values were lower than 0.4, the $LaNi_{1-x}Cr_xO_3$ perovskite catalysts were decomposed to La_2O_3 and Ni and the decomposition of perovskite structure led to large coke deposition. When the x values were higher than 0.4, the $LaNi_{1-x}Cr_xO_3$ perovskite catalysts showed reduced catalytic activity but became stable to reduction and coke formation in the reforming reaction.

Key words: CO_2 Reforming, Methane, Perovskite, Synthesis Gas

INTRODUCTION

Carbon dioxide reforming of methane (the so-called dry reforming) to synthesis gas has received increasing attention from both environmental and industrial perspectives. To reduce the emission of carbon dioxide, a representative greenhouse gas causing the global-warming problem, the carbon dioxide reforming reaction has been considered as an ideal scheme because it can utilize the carbon dioxide to produce valuable synthesis gas. The synthesis gas produced from the carbon dioxide reforming reaction has low ratio of hydrogen to carbon monoxide and it is suitable for the production of long-chain hydrocarbons in the Fischer-Tropsch synthesis process [1,2]. Also, the reactants for the carbon dioxide reforming reaction, methane (CH_4) and carbon dioxide (CO_2), are cheap and abundant carbon-containing components; therefore, the reaction process is economically feasible [3-13].

$$CH_4+CO_2 \rightarrow 2H_2+2CO,\ \Delta H^{o}_{298\,K}=247\ kJ/mol \quad (1)$$

The CO_2 reforming reaction, Eq. (1), is intensively endothermic, so it should be operated at high temperatures. Under such a severe condition, catalysts are easily deactivated by coke deposition and/or sintering of the catalysts. During the past decades, much effort has been focused on the development of catalysts which show high activity towards synthesis gas formation and resistance against coking and sintering for long term operation. Especially, numerous supported metal catalysts were studied for the CO_2 reforming. Among them, nickel-based catalysts [14-21] and supported noble metal catalysts such as Rh, Ru, Ir, Pd, and Pt [22-27] gave promising catalytic performance in terms of activity and selectivity to synthesis gas. Though nickel-based catalysts are reported to be effective, they are easily deactivated by the coke formation. The noble metal catalysts have been found to have resistance against coking, whereas they do not seem to be practical because they are expensive.

Recently, much attention has been paid to perovskite type oxides with the general formula of ABO_3 (where A and B are lanthanide and/or alkaline earth and transition metal cations, respectively) as catalysts which can be substituted for noble metal catalysts in the CO_2 reforming [28,29]. Perovskite oxides have advantages of high catalytic activity and thermal stability. In addition, the high stability of the perovskite structure allows the partial substitution of A and B site cations by other metals. Among them, the lanthanide perovskites, $LaBO_3$ have received the most attention in the CO_2 reforming [13,29-32]. The $LaBO_3$ perovskite catalysts can be improved by partial substitution on A and/or B sites, and the thermodynamic stability of $LaBO_3$ to reduction is known to decrease in the order of B=Cr, Fe, Mn, Co, Ni [33]. In general, the catalytic activity of the perovskite catalysts is related to the reduction behavior. Wu et al. [31] reported that $LaBO_3$ (B=Cr, Fe, Ni, Co) showed increasing catalytic activity in the order of B=Co, Ni, Fe, Cr for the CO_2 reforming of CH_4. However, $LaNiO_3$ and $LaCoO_3$ are easily decomposed to La_2O_3 and metals, which results in a large amount of coke deposition. Partial substitution of transition metal by other trivalent cations can be effective to enhance the catalytic activity and/or stability to reduction [13,29,32].

This paper presents the effects of the partial substitution of Ni by Cr in $LaNiO_3$ perovskite catalyst on the catalytic activity and the stability against coke deposition in the CO_2 reforming of CH_4. X-ray diffractometry and temperature-programmed reduction analysis were used to characterize the reduction of perovskite catalysts, and the catalytic reaction was carried out in a packed column to investigate reaction performance. The partial substitution of Ni by Cr in $LaNiO_3$ perovskite catalyst somewhat reduced the catalytic activity but significantly improved stability to reduction and coke deposition.

†To whom correspondence should be addressed.
E-mail: sihong@korea.ac.kr, kibonglee@korea.ac.kr

EXPERIMENTAL

1. Preparation of $LaNi_{1-x}Cr_xO_3$ Catalysts

Lanthanum nickel chromium oxide, $LaNi_{1-x}Cr_xO_3$, with different composition (x=0, 0.2, 0.4, 0.6, 0.8, 1.0) was prepared by the malic acid method as reported in the literature [34]. The required amount of metal nitrate in stoichiometric ratio was dissolved in water to which malic acid was added. The molar ratio of malic acid to total metal ions was set at 1.5. The pH of solution was adjusted by dropwise addition of aqueous ammonia and nitric acid into the mixed aqueous solution with stirring. Then, most water in the solution was removed by heating at 80 °C and the resulting viscous solution was heated at 100 °C for further drying. Additional heating to 210 °C in a drying oven caused a thermal decomposition of precursor, and NO_2 and other gases were produced during the decomposition of precursor. In this process, the perovskite oxide precursor was formed as solid foam, which was ground up using a jade mortar and pestle. Afterward, the precursor powder was calcined at 900 °C for 2 h in air. The formation of the perovskite phase was confirmed by powder X-ray diffraction (XRD).

2. Catalysts Characterization

XRD patterns of perovskite catalysts were recorded with a Rigaku X-ray diffractometer (Rigaku D/Max-III C) with Cu Kα radiation operated at 40 kV and 100 mA. The scan range was from 20° to 80° 2θ. XRD analysis was performed to identify crystal structures. The surface area of the perovskite catalysts was determined by nitrogen adsorption, by using a Micrometrics ASAP 2010 instrument. The sample was degassed at 200 °C in high vacuum before measurement. The surface area was calculated by the Brunauer-Emmett-Teller (BET) method. The morphology of coke produced in the CO_2 reforming was investigated with a Philips CM30 transmission electron microscope (TEM) operated at 200 kV. The sample for TEM analysis was prepared by suspending a small amount of catalyst in ethanol followed by sonication. One drop of this suspension was put on a carbon-coated copper grid and dried.

3. Temperature-programmed Reduction

Temperature-programmed reduction (TPR) of catalyst was carried out by using 10% hydrogen balanced by nitrogen as reducing gas. Gas flow rate was fixed at 30 mL/min and adjusted by mass flow controllers. Hydrogen consumption in the TPR was detected by a thermal conductivity detector (TCD) and its signal was transferred to a personal computer. The peak areas of TPR data could be separated and integrated by a computer software program. The temperature of the catalyst sample was controlled by a temperature-programmable controller. The cell used for TPR was made of 6 mm-I.D. quartz tube and the catalyst sample was mounted on loosely packed quartz wool. The outlet from the TPR cell was connected to a glass column packed with molecular sieve 5A in order to remove moisture produced from reduction procedure. The sample weight was 0.1 g and the heating rate of TPR was 5 °C/min.

4. CO_2 Reforming of CH_4

The catalytic reaction was carried out at the temperature of 600-850 °C in a flow system using a vertical quartz tube (6 mm-I.D.) as the reactor. The catalyst powder of 0.05 g was held on quartz wool. A mixture of CH_4 (50%) and CO_2 (50%) from a pre-mixed gas cylinder was supplied to the reactor. The total flow rate of reactants was set at 60 mL/min and the total pressure was 101.3 kPa. The reactant and product gases were analyzed by two different gas chromatographs equipped with a TCD. The first one (Shimadzu 14A), equipped with Porapak Q column and using He as a carrier gas, was used to analyze CH_4, CO_2, and CO. The second one (Donam Co.), equipped with the same column and using N_2 as a carrier gas, was used to analyze H_2.

RESULTS AND DISCUSSION

1. Characteristics of $LaNi_{1-x}Cr_xO_3$ Perovskite Catalysts

Fig. 1 shows XRD patterns of perovskite catalysts, $LaNi_{1-x}Cr_xO_3$ (x=0, 0.2, 0.4, 0.6, 0.8, 1.0), which were prepared by the malic acid method. $LaCrO_3$ and $LaNiO_3$ had orthorhombic and rhombohedral structures, respectively, at room temperature. The $LaNi_{1-x}Cr_xO_3$ had the orthorhombic $LaCrO_3$ structure for $x \geq 0.4$ and the rhombohedral $LaNiO_3$ structure for $x < 0.4$. This is similar to the result reported by Stojanovic et al. [30] based on the variation of lattice parameters with composition. No impurity phases such as La_2O_3 and Ni were detected in the XRD patterns. Perovskite type structure was preserved with the substitution of B-site element.

Table 1 presents the BET surface area of $LaNi_{1-x}Cr_xO_3$ perovs-

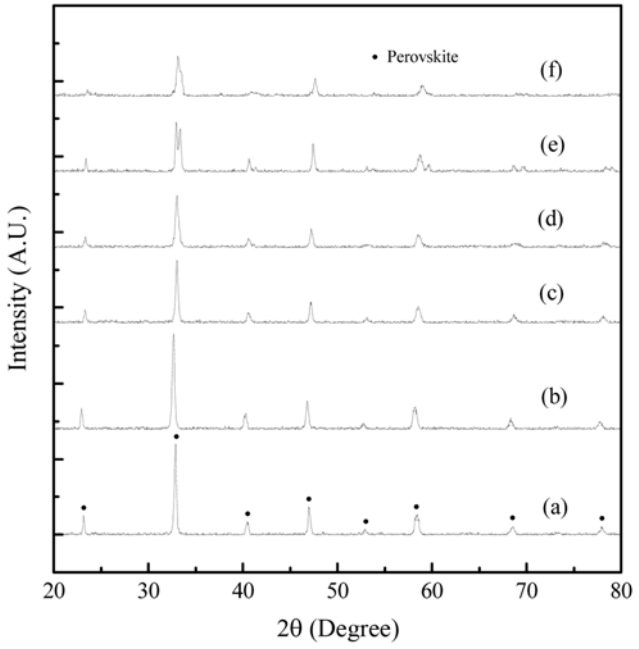

Fig. 1. XRD spectra of $LaNi_{1-x}Cr_xO_3$ perovskite oxides calcined at 900 °C for 2 h, (a) x=1.0, (b) x=0.8, (c) x=0.6, (d) x=0.4, (e) x=0.2, (f) x=0.

Table 1. Specific surface area and apparent activation energy of $LaNi_{1-x}Cr_xO_3$ for CO_2 reforming of CH_4

Catalyst	Specific surface area (m^2/g), calcined at 900 °C	E_{app} (kJ/mol) for CH_4	E_{app} (kJ/mol) for CO_2
$LaNi_{0.8}Cr_{0.2}O_3$	20.3	116.8	118.0
$LaNi_{0.6}Cr_{0.4}O_3$	22.2	115.1	113.0
$LaNi_{0.4}Cr_{0.6}O_3$	25.5	111.3	110.0
$LaNi_{0.2}Cr_{0.8}O_3$	26.3	107.1	104.2

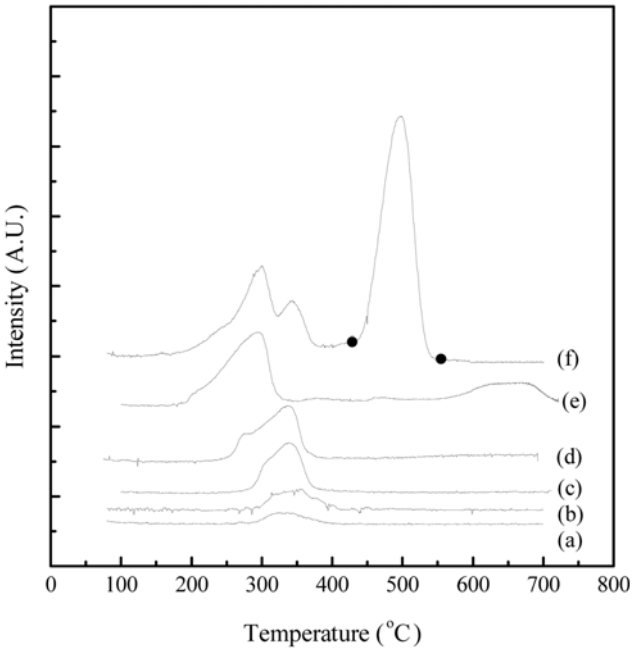

Fig. 2. TPR spectra of $LaNi_{1-x}Cr_xO_3$, (a) x=1.0, (b) x=0.8, (c) x=0.6, (d) x=0.4, (e) x=0.2, (f) x=0 (heating rate: 5 °C/min, purge gas: 10% H_2 balanced by N_2).

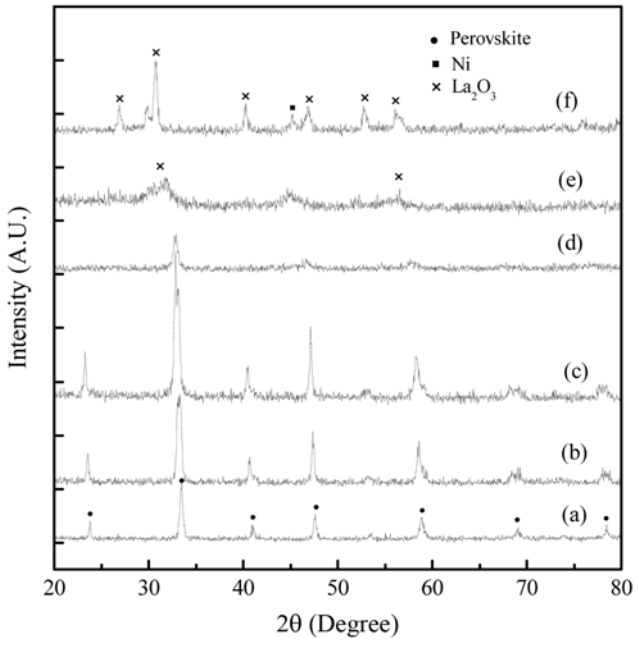

Fig. 3. XRD spectra of $LaNi_{1-x}Cr_xO_3$ perovskite oxides reduced in 20% H_2 at 800 °C for 2 h (a) x=1.0, (b) x=0.8, (c) x=0.6, (d) x=0.4, (e) x=0.2, (f) x=0.

kite catalysts. When Ni and Cr coexisted in the perovskite catalysts, the surface area of catalysts increased with increasing Ni substitution by Cr.

2. Reduction Behavior in Hydrogen

It is well known that the oxygen species of perovskite catalyst plays an important role in the catalytic oxidation reaction. Also, the stability of perovskite oxide structure under reducing condition is related to the strength of bulk lattice oxygen bonds. To characterize the oxygen species in perovskite oxide, TPR tests were performed.

Fig. 2 shows TPR spectra of $LaNi_{1-x}Cr_xO_3$ (x=0, 0.2, 0.4, 0.6, 0.8, 1.0). In the TPR procedure, $LaNiO_3$ was reduced in two steps. The first reduction peak of $LaNiO_3$ occurred at 300 °C with a high temperature shoulder at 340 °C. This peak was caused by the reduction of adsorbed oxygen or surface lattice oxygen of perovskite oxide. This corresponds to the reduction of Ni^{3+} into Ni^{2+}. The second peak occurred at 490 °C and corresponds to complete reduction to La_2O_3 and Ni by the reduction of bulk lattice oxygen [35,36]. On the other hand, $LaCrO_3$ was reduced slightly at 340 °C. Fierro and Tejuca [35] studied oxygen species of $LaMO_3$ (M=Cr, Mn, Fe, Co, Ni) by X-ray photoelectron spectroscopy measurements and found that the peak at low binding energy corresponded to the surface lattice oxygen, which can be reduced easily under reducing condition. The peak at high binding energy corresponded to the bulk lattice oxygen, which is more stable to reduction. In the change from $LaNiO_3$ to $LaCrO_3$, the peak at high binding energy increased in intensity and shifted to higher binding energy.

All perovskite catalysts used in our experiments were reduced at 300-340 °C, which corresponds to the change of Ni^{3+} to Ni^{2+}. As more Cr was substituted in $LaNiO_3$, the degree of reduction was decreased. For x=0.2, the second peak was shifted to the higher temperature region, ca. 650 °C, and the degree of reduction of bulk lattice oxygen was decreased as aforementioned. For x≥0.4, the second peak did not appear, and this behavior corresponds to the perovskite structure which becomes stable under reducing condition.

Fig. 3 shows the XRD patterns of the reduced $LaNi_{1-x}Cr_xO_3$ perovskite oxides under 20% H_2 at 800 °C for 2 h. For x≥0.4, $LaNi_{1-x}Cr_xO_3$ perovskite oxides had their intrinsic crystal structure. However, when x<0.4, $LaNi_{1-x}Cr_xO_3$ perovskite oxides underwent a drastic structural change to La_2O_3 and Ni. These XRD results agreed well with the above-mentioned TPR results.

3. Catalytic Activity

To investigate catalytic activity of $LaNi_{1-x}Cr_xO_3$ perovskite catalysts, CO_2 reforming of CH_4 was performed at 600-850 °C and 101.3 kPa. A mixture of CH_4 and CO_2 with the ratio of CH_4/CO_2=1.0 was used as the reactant and the space velocity was fixed at 7.2×10^4 $cm^3/g\cdot h$. Figs. 4 and 5 show the conversion over $LaNi_{1-x}Cr_xO_3$ perovskite catalysts as a function of reaction temperature and the Arrhenius plots of the CO_2 reforming based on CH_4 and CO_2 components, respectively. As the reaction temperature increased, both CH_4 and CO conversions increased significantly at around 700 °C and then slowly at around 800 °C. The catalytic activity was also increased with increasing Ni content in $LaNi_{1-x}Cr_xO_3$. The catalytic activity of perovskite in the CO_2 reforming is related to the surface oxygen species of catalysts, and $LaNiO_3$ is more active than $LaCrO_3$ because Ni is a more reducible transition metal. Wu et al. [31] reported that the CO_2 reforming catalytic activity of $LaMO_3$ at 800 °C followed the order of $LaCoO_3$>$LaNiO_3$>$LaFeO_3$>$LaCrO_3$. However, both $LaNiO_3$ and $LaCoO_3$ were decomposed in the CO_2 reforming, and $LaCrO_3$ was very stable under reducing condition.

For nickel-rich perovskite catalysts (x<0.4), the bulk lattice oxygen as well as the surface oxygen was reduced easily. The catalytic activity of $LaNiO_3$ was high but the structure was unstable under reducing condition owing to its reduction behavior. On the other hand, $LaCrO_3$ had low catalytic activity but was very stable to reduc-

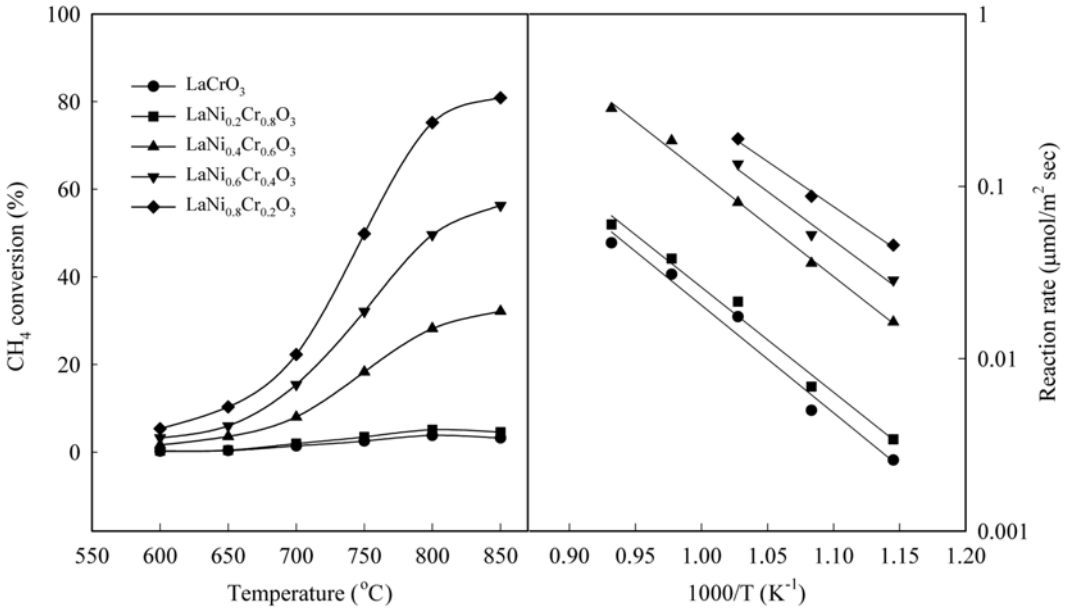

Fig. 4. Effect of reaction temperature on CH_4 conversion and the Arrhenius plot based on CH_4 conversion over $LaNi_{1-x}Cr_xO_3$ perovskite catalysts (CH_4/CO_2=1.0, GHSV=72.0 $cm^3/kg \cdot h$).

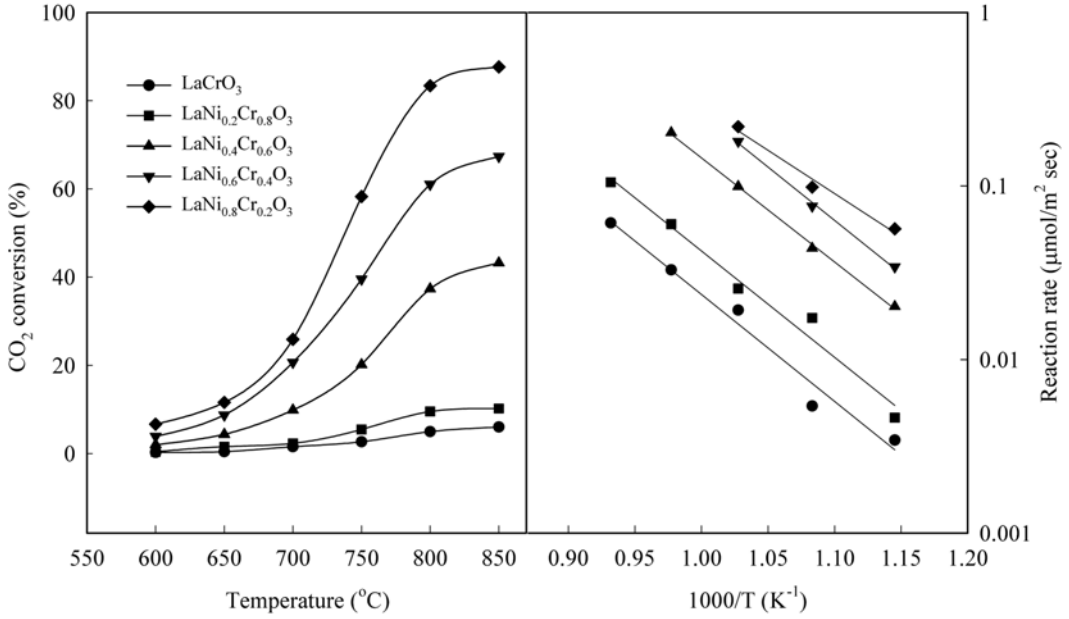

Fig. 5. Effect of reaction temperature on CO_2 conversion and the Arrhenius plot based on CO_2 conversion over $LaNi_{1-x}Cr_xO_3$ perovskite catalysts (CH_4/CO_2=1.0, GHSV=72.0 $cm^3/kg \cdot h$).

tion (Fig. 2). The increase of Cr content in the $LaNi_{1-x}Cr_xO_3$ perovskite led to more strongly bonded oxygen species, which were more stable to reduction and resulted in persistent catalytic activity.

The apparent activation energies for CH_4 and CO_2 over $LaNi_{1-x}Cr_xO_3$ perovskite catalysts in CO_2 reforming are shown in Table 1. The apparent activation energy was decreased with increasing Cr content in the $LaNi_{1-x}Cr_xO_3$ perovskite.

Fig. 6 shows the effect of the partial substitution of Ni by Cr in $LaNiO_3$ on the conversion and selectivity in the CO_2 reforming to synthesis gas at 800 °C. Both conversion and selectivity for H_2 were increased with increasing Ni content in $LaNi_{1-x}Cr_xO_3$ perovskite catalysts. However, with increasing Ni content, the selectivity for CO was reduced, which implies that coke formation in the CO_2 reforming occurred according to the Boudouard reaction ($2CO \rightarrow C+CO_2$). In the overall reaction experiments, the conversion of CO_2 was higher than that of CH_4. This could be caused by the reverse water gas shift reaction ($CO_2+H_2 \rightarrow CO+H_2O$), where the H_2 produced from the CO_2 reforming reaction further reacts with CO_2 [31]. Therefore, more CO_2 could be consumed in the reaction than expected. In general, the carbon in the feed reactants can be changed into C, CO, and CO_2. To investigate the coke formation, long-term operation was carried out as shown in Section 4.

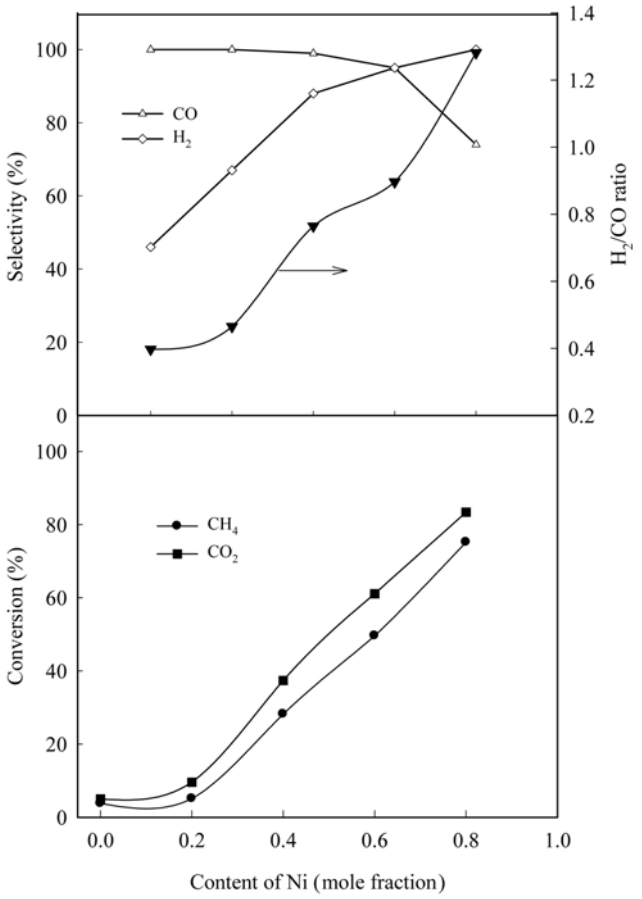

Fig. 6. Effect of Ni content in $LaNi_{1-x}Cr_xO_3$ perovskite catalysts on conversion, selectivity, and H_2/CO ratio in the CO_2 reforming at 800 °C (CH_4/CO_2=1.0, GHSV=72.0 $cm^3/kg \cdot h$).

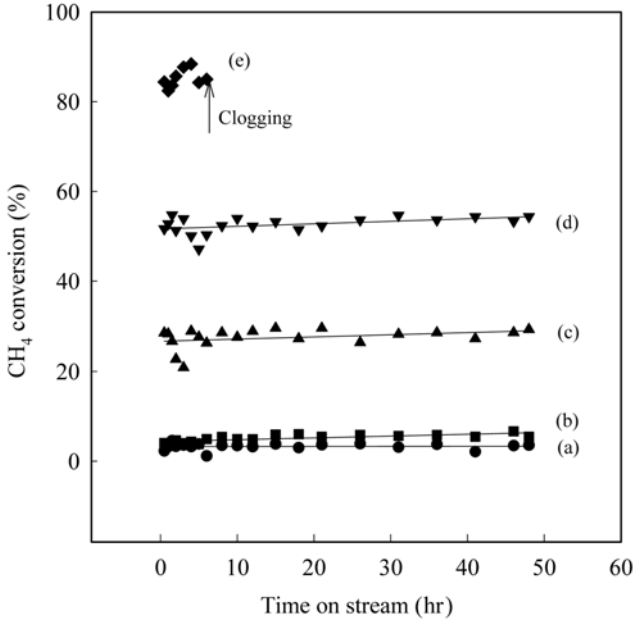

Fig. 7. CH_4 conversions with time-on-stream in the CO_2 reforming over $LaNi_{1-x}Cr_xO_3$ perovskite catalysts at 800 °C (a) x=1.0, (b) x=0.8, (c) x=0.6, (d) x=0.4, (e) x=0.2 (CH_4/CO_2=1.0, GHSV=72.0 $cm^3/kg \cdot h$).

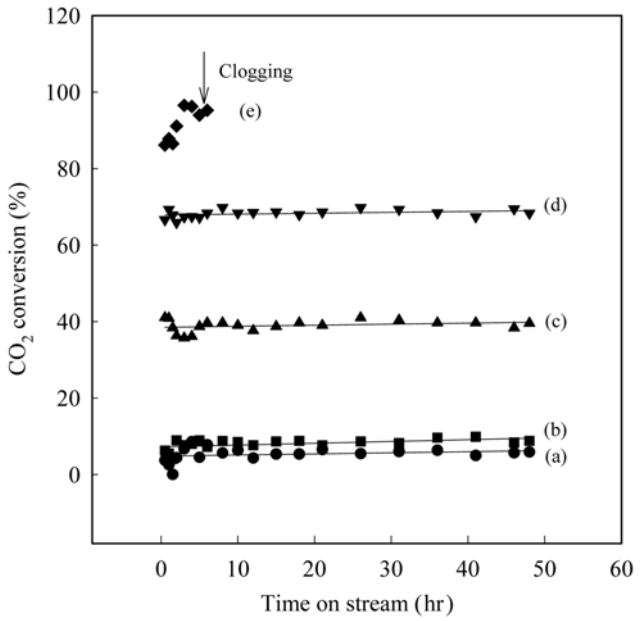

Fig. 8. CO_2 conversions with time-on-stream in the CO_2 reforming over $LaNi_{1-x}Cr_xO_3$ perovskite catalysts at 800 °C (a) x=1.0, (b) x=0.8, (c) x=0.6, (d) x=0.4, (e) x=0.2 (CH_4/CO_2=1.0, GHSV=72.0 $cm^3/kg \cdot h$).

4. Time-on-stream Stability in CO_2 Reforming of CH_4

Figs. 7 and 8 show the conversions of CH_4 and CO_2 over $LaNi_{1-x}Cr_xO_3$ perovskite catalysts with time-on-stream in the CO_2 reforming at 800 °C. For nickel-rich perovskite catalysts (x<0.4), the initial activity was very high, but coke was rapidly deposited after the CO_2 reforming reaction started. The nickel-rich perovskite catalysts were easily reduced to La_2O_3 and Ni (evidenced by XRD analysis in Fig. 3) in the CO_2 reforming reaction, and the catalytic activity was increased as the decomposition proceeded. After the catalyst was completely reduced to La_2O_3 and Ni, the catalytic activity was more active but the stability against coking became very poor. For the CO_2 reforming over nickel-rich perovskite catalysts (x<0.4), a rapid pressure drop occurred in the plug flow reactor by clogging after 4 h operation. For the $LaNi_{1-x}Cr_xO_3$ perovskite catalysts of x≥0.4, the catalysts were stable and the catalytic activities were maintained constantly in the CO_2 reforming for 48 h. As shown in the TPR results (Fig. 2), the bulk lattice oxygen was stable to reduction. The partial substitution of Ni by Cr in the $LaNi_{1-x}Cr_xO_3$ led to the increased M-O bond strength, resulting in good stability to reduction and coke deposition.

The amount of coke produced on the perovskite catalysts in the CO_2 reforming was measured by thermogravimetric analysis (TGA). Thermogravimetric oxidation of the used catalysts was performed at 5 °C/min in air. Table 2 shows the TGA results of the catalysts used in the CO_2 reforming at 800 °C. $LaNiO_3$ and $LaNi_{0.8}Cr_{0.2}O_3$ catalysts showed very poor resistance to coke formation. However, in the $LaNi_{1-x}Cr_xO_3$ perovskite catalysts of x≥0.4, coke formation was remarkably reduced even after 48 h operation. In the reforming reaction, the coke formation was known to be attributed to nickel metal size and metal interaction with its supporter [37]. The nickel-rich perovskite catalysts (x<0.4) were reduced into La_2O_3 and Ni, as shown in the XRD data (Fig. 3), and the reduced nickel was sin-

Table 2. Effect of the Cr content in perovskite catalysts on coke deposition under CO_2 reforming of CH_4

Catalyst	Amount of coke formation (%)
$LaNi_{0.2}Cr_{0.8}O_3$	0.04
$LaNi_{0.4}Cr_{0.6}O_3$	0.91
$LaNi_{0.6}Cr_{0.4}O_3$	0.05
$LaNi_{0.8}Cr_{0.2}O_3$	47.4
$LaNiO_3$	67.8

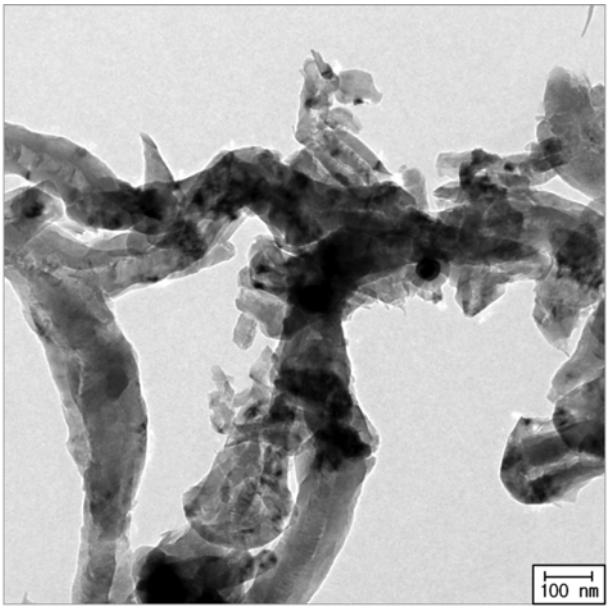

Fig. 9. TEM image of deposited coke on $LaNi_{0.8}Cr_{0.2}O_3$ after the CO_2 reforming reaction.

tered in the CO_2 reforming, resulting in severe coke formation. Fig. 9 shows the TEM image of deposited coke on $LaNi_{0.8}Cr_{02}O_3$ in the CO_2 reforming. It is apparent that there were encapsulated carbons as well as whisker carbons. The whisker carbons were estimated to be 20-30 nm in diameter. Trimm [38] reported that the reaction of hydrocarbons as well as carbon oxides over Ni catalysts can lead to the formation of the filamentous carbons, and the carbons grow in a whisker structure associated with nickel particle. The chromium-rich perovskite catalysts ($x \geq 0.4$), leading to the increase of M-O bond strength, suppressed the formation of large nickel particle on the surface and thus avoided coke formation.

CONCLUSIONS

$LaNi_{1-x}Cr_xO_3$ (x=0, 0.2, 0.4, 0.6, 0.8, 1.0) perovskite catalysts were investigated for CO_2 reforming of CH_4. The catalytic behavior was related to the characteristics of the reduction behavior. For $x<0.4$ in $LaNi_{1-x}Cr_xO_3$, the perovskite catalysts were highly active but easily decomposed to La_2O_3 and Ni, which led to large coke deposition. For $x \geq 0.4$ in $LaNi_{1-x}Cr_xO_3$, the perovskite catalysts were stable in the CO_2 reforming. The partial substitution of Ni by Cr in the $LaNi_{1-x}Cr_xO_3$ perovskite catalysts enhanced M-O bond strength and resulted in the good stability to reduction and coke deposition.

The composition of $LaNi_{1-x}Cr_xO_3$ perovskite catalyst should be optimized with respect to the catalytic activity and the stability to coke deposition. Among the perovskite catalysts tested in this study, $LaNi_{0.6}Cr_{0.4}O_3$ showed reasonable catalytic activity and good stability against the coke deposition in the CO_2 reforming to synthesis gas.

ACKNOWLEDGEMENTS

This work was supported by the Human Resources Development program of the Korea Institute of Energy Technology Evaluation and Planning (KETEP) grant funded by the Korean government's Ministry of Knowledge Economy (No. 20114010203050) and the Development of Biohydrogen Production Technology Using Hyperthermophilic Archaea Program of the Korean government's Ministry of Land, Transport, and Maritime Affairs.

REFERENCES

1. Y. H. Hu and E. Ruckenstein, *Adv. Catal.*, **48**, 297 (2004).
2. M. S. Fan, A. Z. Abdullah and S. Bhatia, *ChemCatChem*, **1**, 192 (2009).
3. A. T. Ashcroft, A. K. Cheetham, M. L. H. Green and P. D. F. Vernon, *Nature*, **452**, 225 (1991).
4. J. M. Fox, *Catal. Rev. Sci. Eng.*, **35**, 169 (1993).
5. J. R. Rostrup-Nielsen and J. H. B. Hansen, *J. Catal.*, **144**, 38 (1993).
6. Z. Zhang and X. E. Verykios, *J. Chem. Soc., Chem. Commun.*, 71 (1995).
7. Y. H. Hu and E. Ruckenstein, *J. Catal.*, **163**, 306 (1996).
8. R. N. Bhat and W. M. H. Sachtler, *Appl. Catal. A: Gen.*, **150**, 279 (1997).
9. H. Y. Wang and C. T. Au, *Appl. Catal. A: Gen.*, **155**, 239 (1997).
10. S. M. Stagg, E. Romeo, C. Padro and D. E. Resasco, *J. Catal.*, **178**, 137 (1998).
11. M. C. J. Bradford and M. A. Vannice, *J. Catal.*, **183**, 69 (1999).
12. M. C. J. Bradford and M. A. Vannice, *Catal. Rev. Sci. Eng.*, **41**, 1 (1999).
13. G. C. de Araujo, S. M. de Lima, J. M. Assaf, M. A. Pena, J. L. G. Fierro and M. C. Rangel, *Catal. Today*, **133-135**, 129 (2008).
14. Y. G. Chen and J. Ren, *Catal. Lett.*, **29**, 39 (1994).
15. V. R. Choudhary, B. S. Uphade and A. S. Mamman, *Catal. Lett.*, **32**, 387 (1995).
16. V. R. Choudhary, B. S. Uphade and A. A. Belhekar, *J. Catal.*, **163**, 312 (1996).
17. Z. L. Zhang, X. E. Verykios, S. M. MacDonald and S. J. Affrossman, *J. Phys. Chem.*, **100**, 744 (1996).
18. Z. L. Zhang and X. E. Verykios, *Appl. Catal. A: Gen.*, **138**, 109 (1996).
19. Z. Cheng, Q. Wu, J. Li and Q. Zhu, *Catal. Today*, **30**, 147 (1996).
20. V. R. Choudhary and A. M. Rajput, *Ind. Eng. Chem. Res.*, **35**, 3934 (1996).
21. H. Kim, S. J. Lee and K. S. Song, *Korean J. Chem. Eng.*, **24**, 477 (2007).
22. F. Solymosi, G. Kutsan and A. Erdohelyi, *Catal. Lett.*, **11**, 149 (1991).
23. A. Erdohelyi, E. Cserényi and F. Solymosi, *J. Catal.*, **141**, 287 (1993).
24. D. Qin and J. Lapszewicz, *Catal. Today*, **21**, 551 (1994).
25. M. F. Mark and W. F. Maier, *J. Catal.*, **164**, 122 (1996).
26. K. Nagaoka, K. Takanabe and K. Aika, *Appl. Catal. A: Gen.*, **268**,

151 (2004).
27. Z. Y. Hou, P. Chen, H. L. Fang, X. M. Zheng and T. Yashima, *Int. J. Hydrog. Energy*, **31**, 555 (2006).
28. A. Sauvet, J. Guindet and J. Fouletier, *IONICS*, **5**, 150 (1999).
29. M. E. Rivas, J. L. G. Fierro, M. R. Goldwasser, E. Pietri, M. J. Pérez-Zurita, A. Griboval-Constant and G. Leclercq, *Appl. Catal. A: Gen.*, **344**, 10 (2008).
30. M. Stojanovic, R. G. Haverkamp, C. A. Mims, H. Moudallal and A. J. Jacobson, *J. Catal.*, **166**, 315 (1997).
31. Y. Wu, O. Kawaguchi and T. Matsuda, *Bull. Chem. Soc. Jpn.*, **71**, 563 (1998).
32. G. Valderrama, A. Kiennemann and M. R. Goldwasser, *Catal. Today*, **133-135**, 142 (2008).
33. T. Nakamura, G. Petzow and L. J. Gauckler, *Mater. Res. Bull.*, **14**, 649 (1979).
34. J. W. Erning, T. Hauber, U. Stimming and K. Wippermann, *J. Power Sources*, **61**, 205 (1996).
35. J. L. G. Fierro and L. G. Tejuca, *Appl. Surf. Sci.*, **27**, 453 (1987).
36. L. G. Tejuca and J. L. G. Fierro, *Thermochim. Acta*, **147**, 361 (1989).
37. H. Provendier, C. Petit, C. Estournes, S. Libs and A. Kiennemann, *Appl. Catal. A: Gen.*, **180**, 163 (1999).
38. D. L. Trimm, *Catal. Rev. Sci. Eng.*, **16**, 155 (1977).